Test-case number 2: Free rise of a liquid inclusion in a stagnant liquid (PN, PE)

July 16, 2002

Hervé Lemonnier, DER/SSTH/LIEX, CEA/Grenoble, 38054 Grenoble cedex 9, France
Phone: +33 (0)4 38 78 45 40, Fax: +33 (0)4 38 78 50 45, E-Mail: *herve.lemonnier@cea.fr*

Eric Hervieu, DER/SSTH/LIEX, CEA/Grenoble, 38054 Grenoble cedex 9, France
Phone: +33 (0)4 38 78 45 33, Fax: +33 (0)4 38 78 50 45, E-Mail: *eric.hervieu@cea.fr*

1 Practical significance and interest of the test-case

A numerical solution of a free boundary problem and a related experiment are provided here. The experiment is devoted to the stability of an inclusion rising freely under the sole action of gravity, a situation which is known to depend critically on the initial conditions in a non-linear way. In particular, there exists a *critical capillary number* beyond which a rising inclusion becomes unstable and this critical value depends non linearly on the shape of the inclusion. When the instability occurs, very high curvatures are experienced by the interface the motion of which results only from the equilibrium between surface tension effects and viscous shear stresses. This situation represents a very severe test of the description of surface tension and viscous stresses at the interface for solvers dealing with interfaces. The challenge consists here in predicting accurately the critical capillary number beyond which an initially distorted inclusion does not recover its equilibrium spherical shape. An analytical description of the initial inclusion shape of the related experiments is provided to ease further comparison of the results.

When the motions are very slow such as those occurring in very viscous fluids, the inner and outer flows may be described by the steady restriction of the Stokes equations. As a result of the disappearance of non-linear terms in the equation of motion, there exists a boundary element method (BEM) formulation of the problem which only requires to discretize the common interface of the two fluids (**????**). When in addition the flows own a cylindrical symmetry further reduction of the mathematical burden results and the model describes very accurately the experiments (**?**) at a relatively low computing cost.

2 Definitions and model description

The situations to be considered are relative to a liquid inclusion moving in another liquid. The reference calculations to be proposed are made in non-dimensional units. The length scale of the problem is the radius of the sphere the volume of which is equal to that of the initial shape of the inclusion. For a prolate ellipsoid the equivalent radius R is related to the two principal axis of the ellipsoid by,

$$R = \sqrt[3]{a_z a_R^2}, \tag{1}$$

where a_z is the length of the axis in the z direction which is the symmetry axis of the cylindrical coordinate system and a_r is the length of the axis in the radial direction. For a spherical inclusion rising freely under the action of buoyancy forces, the rise velocity has been calculated exactly by Hadamard and Rybczynski within the Stokes approximation

(**?**, p. 184). It reads,

$$U = \frac{2}{3} \frac{R^2|\rho_O - \rho_I|g}{\mu_O} \frac{1+\lambda}{3+2\lambda}, \tag{2}$$

where ρ is the density, μ is the dynamic viscosity, g is the acceleration of the gravity, the subscripts I and O denote respectively the inner and the outer fluid and λ is the ratio of the outer to the inner fluid viscosity given by,

$$\lambda = \frac{\mu_O}{\mu_I}. \tag{3}$$

The Hadamard rise velocity is the velocity scale of the problem (**?**). The non-dimensional problem is therefore completely determined by the ratio of the fluids viscosity and a capillary number measuring the effect of viscous shear on the interface which induces the deformation of the inclusion the scale of which is $\mu_0 U/R$ and the restoring effect of the surface tension which resists to its distortion. The scale of the latter is σ/R (**?**). This capillary number is defined by,

$$Ca = \frac{\mu_O U}{\sigma}, \tag{4}$$

where σ is the surface tension. It is reminded that the Stokes approximation is valid when the Reynolds number relative to each fluid is very small,

$$Re = \frac{\rho U R}{\mu} \ll 1. \tag{5}$$

It must be noted that the time scale of the problem, τ, is therefore,

$$\tau = \frac{R}{U}. \tag{6}$$

During an experiment the volume of the inclusion can be controlled and is measured. Therefore, the equivalent radius R is given. The initial shape can be measured or controlled. If a prolate ellipsoid is considered as an initial shape, then the ratio of its two axis, a_z/a_r is given. Finally the physical properties of each fluid and the interface are known, *i. e.* ρ_O, ρ_I, μ_O, μ_I and σ.

3 A series of six numerical test-cases

It is proposed to calculate the evolution of the shape of an ellipsoid initially at rest rising in another liquid of infinite extent according to the parameters of table 1. It is required to compare the shapes at the non-dimensional times shown in the caption of the figures 1 and 2 selected from the simulations presented by **?**. The shapes must be plotted every 2 non-dimensional time units and the simulation stops when the spherical shape is recovered or when the instability is fully developed.

It is also required to compare the non-dimensional time when the instability is fully developed, *i. e.* the time when some of the inner fluid is entirely encapsulated in the inclusion (see figure 2) or when a fragment detaches from the main body (see figure 1). These times are indicated in the figures captions.

The reference solution has been calculated by utilizing a boundary elements method derived for the Stokes equation. It is to be noted that these results have been reproduced

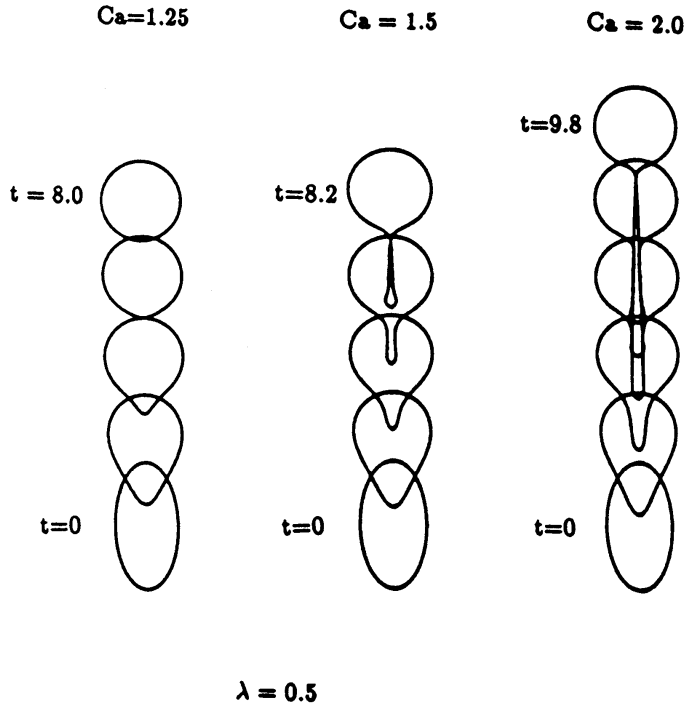

Figure 1: Numerical simulation of the evolution of an initially elongated (prolate) ellipsoid. Cases 2.1 to 2.3 of table 1. After the figure 1 of ?.

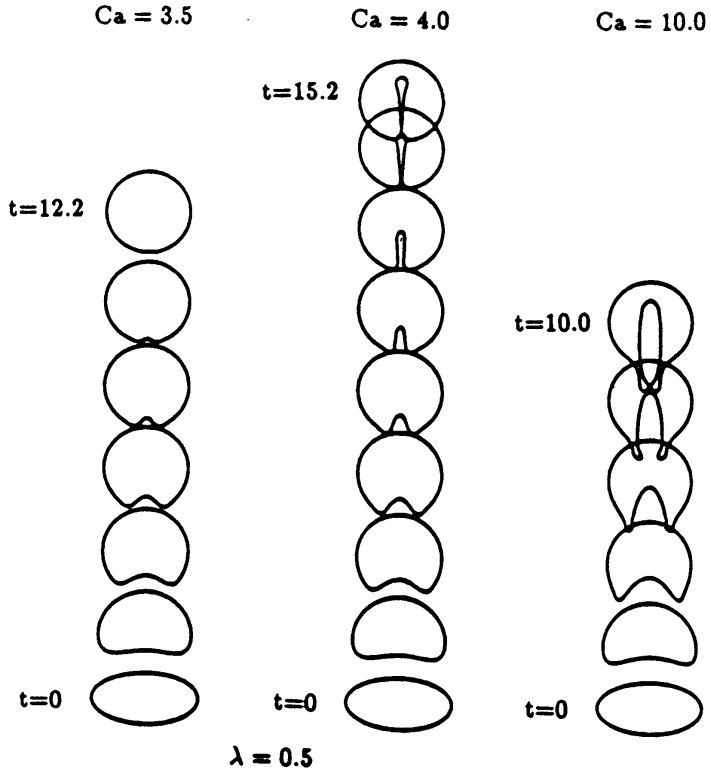

Figure 2: Numerical simulation of the evolution of an initially blunt (oblate) ellipsoid. Cases 2.4 to 2.6 of table 1. After the figure 5 of ?.

Test-case	a_z/a_R	Ca	λ
2.1	2	1.25	0.5
2.2	2	1.5	0.5
2.3	2	2	0.5
2.4	0.5	3.5	0.5
2.5	0.5	4	0.5
2.6	0.5	10	0.5

Table 1: Values of the non-dimensional parameters describing the simulations by **?** presented in figures 1 and 2. The definitions of the non-dimensional parameters are given in section 2.

by **?** and **?** who reported only insignificant differences at the latest times with the original calculations published by **?**. The proposed simulations can therefore be regarded as *exact* solutions to the problem.

The precision of the simulation can also be appreciated by comparing the free rise of a spherical drop to the theoretical value given by Hadamard (2). **?** reported that in their calculations, the velocity of all the points on the interface was within $\pm 0.05\%$ of this theoretical value. The mean value and standard deviation on the interface values of the velocity are acceptable criteria.

Fluid	viscosity (Pa s)	density (kg/m^3)	superficial tension (N/m)
outer	39.1	1021	
inner #1	1.02	972	$5.8\ 10^{-3}$
inner #2	10.1	972	$6.0\ 10^{-3}$
inner #3	29.1	972	$5.8\ 10^{-3}$
inner #4	102	975	$5.8\ 10^{-3}$

Table 2: Values of the physical properties in S. I. units of the experiments by **?**. The superficial tension is to be considered between the outer fluid and each inner fluid.

It is acknowledged that most of the simulation tools do not utilize non-dimensional units. As a result, some preprocessing of the data may be necessary to find a physical situation corresponding to the non-dimensional test-cases of the figures 1 and 2. Some physical properties extracted from the experimental work of **?** may help in identifying these situations. It must be noted that with these values and a drop with an initial volume ranging from 1 to 10 cm^3 the Reynolds number is always less than 10^{-2} and the capillary number ranges from 1 to 5.5.

Summary of the required calculations

- The mean and standard deviation of the velocity at the interface of a spherical inclusion rising in Stokes regime for $\lambda = 10$, 1 and 0.1.
- The shapes of inclusions according to table 1 every 2 non-dimensional time units.
- The time at which the instability is fully developed for the cases of table 1.

4 An experimental test-case

? made a series of experiments in conditions close to those of **?**. Among them,

prolate cases have been selected since they do not cause any interpretation difficulties. Oblate cases ends up with some inner fluid encapsulation where refraction distorts the inner fluid boundary. The prolate inclusions are not prone to this visualization artifact.

It is required to calculate the evolution of the shape of the inclusion as described in figure **??** at time t=0, at the later times t=2.9, 5.4, 8.5, 12.3 and 14.8 s. The physical properties relative to this experiment are given in table **??**. The experiments where conducted in silicone oil (1000 cS) the viscosity of which is comparable with the inner fluid number 1 of **?**. The inner fluid was a blend of castor oil and 3% in volume of methanol. The initial shape is given in table **??** and an analytical approximation is proposed in the appendix for the sake of simplicity.

Fluid	viscosity (Pa s)	density (kg/m^3)	superficial tension (N/m)
outer	0.988	970	
inner	0.593	953	$3.8\ 10^{-3}$

Table 3: Values of the physical properties in S. I. units of the experiments by **?**. The superficial tension is to be considered between the outer fluid and the inner fluid.

Z (mm)	R (mm)	Z (mm)	R (mm)	Z (mm)	R (mm)
20.09	0.00	6.49	9.97	-7.31	6.65
19.31	3.75	5.39	9.91	-8.29	6.33
18.32	5.47	4.52	9.74	-9.37	5.97
17.33	6.61	3.54	9.54	-10.26	5.73
16.35	7.53	2.55	9.31	-11.25	5.40
15.36	8.16	1.56	9.08	-12.23	5.08
14.38	8.66	0.58	8.84	-13.22	4.75
13.39	9.08	-0.41	8.60	-14.20	4.32
12.41	9.42	-1.39	8.39	-15.20	3.98
11.42	9.71	-2.62	8.06	-16.15	3.59
10.43	9.87	-3.52	7.79	-17.74	2.98
9.45	9.92	-4.35	7.57	-18.69	2.49
8.46	9.94	-5.33	7.32	-20.07	1.55
7.48	9.97	-6.26	7.01	-20.90	0.00

Table 4: Coordinates of the initial shape of figure **??**. Lengths are in mm.

It must be noted there exist some sources of uncertainty in the data. The physical properties including the surface tension have been measured in the laboratory by using conventional techniques (**?**). The most uncertain quantity is the density difference between the two fluids. Moreover, the initial velocity of the inclusion is unknown and it may be assumed that it is at rest which is not a too unrealistic assumption owing to the experimental procedure utilized to create elongated inclusions.

Summary of the requested calculations

- The shapes of the inclusion at the times shown in figure **??**.

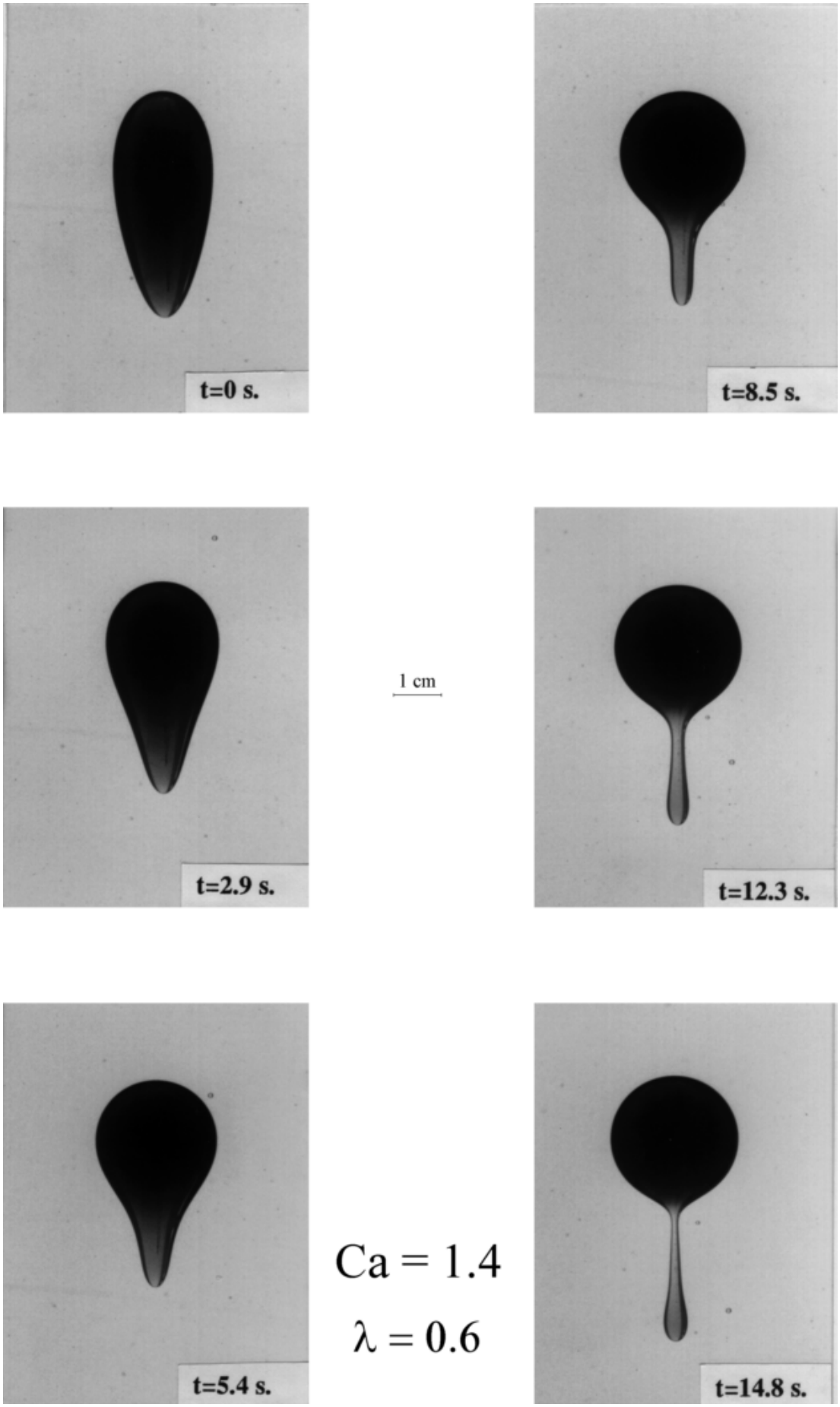

Figure 3: Experiment on the free rise of a liquid inclusion rising in another liquid. Physical properties listed in table **??**. $\lambda = 0.6$, $Ca = 1.4 \pm 0.2$ and $\Delta\rho = 17$ kg/m^3. After **?**

Appendix: an analytical approximation of the initial shape

The data shown in table **??** describing the initial shape of the inclusion shown in figure **??** may be uneasy to handle. **?** used cubic spline functions fitted on nodes sampled from the snapshots of the experiments. The spline functions interpolates respectively the axial and radial coordinate as a function of the curvilinear abscissa along the shape. This method provides the best input for the boundary element method. It has been thought that this procedure may deemed rather cumbersome and unnecessary for most of the solvers. This is the reason why an analytical description of the initial shape is proposed.

The points of table **??** have been transformed by an affine transformation of ratio 2 in the r direction according to **?**. This provides a rather spherical object which can be easily described by trigonometric expansion in polar coordinates according to,

$$r'(\theta) = \sum_{k=0}^{k=8} a_k \cos(k\theta) \tag{7}$$

where the a_k's are given in table **??**. This fit has been performed by the nonlinear least-squares Marquardt-Levenberg algorithm programmed in the `gnuplot` fit function.

order	value (mm)
0	18.9478
1	2.3417
2	1.0630
3	-2.4794
4	0.0268
5	-0.1311
6	0.4327
7	-0.0661
8	-0.0117

Table 5: List of the a_k's in equation (**??**). Unit is mm.

The original coordinates are recovered from the trigonometric expansion (**??**) by the following,

$$\begin{cases} z = r'(\theta)\cos(\theta) \\ r = \frac{1}{2} r'(\theta)\sin(\theta) \end{cases} \tag{8}$$

where the angle θ ranges from 0 to 2π. A comparison of the data and the approximation is shown in figure **??**. A reasonable agreement is noted.

References

Hervieu, E., Coutris, N., & Tavares, M. 1992. Deformation of a fluid particle falling freely in an infinite medium. *Pages 201–207 of: ANS Proc. of 28th National Heat Transfer Conference*. San Diego, CA.

Koh, C. J., & Leal, L. G. 1989. The stability of drop shapes for translation at zero Reynolds number through a quiescent liquid. *Physics of Fluids A*, **1**(8), 1309–1313.

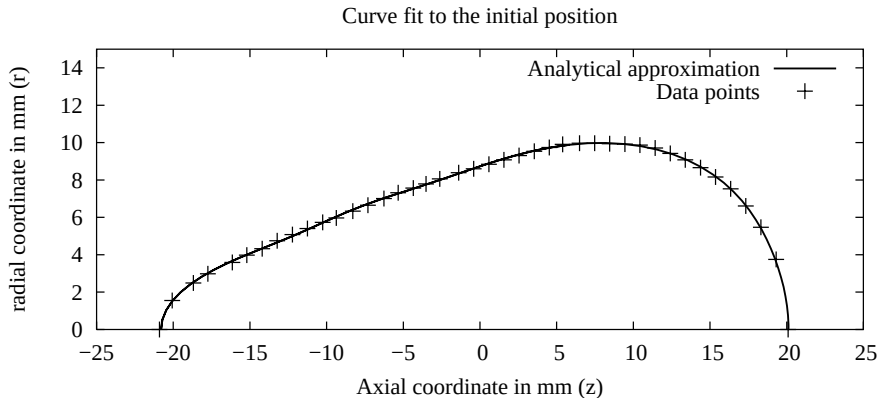

Figure 4: Comparison between the data describing the initial shape in table **??** and the analytic approximation (**??**) and (**??**).

Koh, C. J., & Leal, L. G. 1990. An experimental investigation on the stability of viscous drops translating through a quiescent liquid. *Physics of Fluids A*, **2**(12), 2103–2109.

Mathieu, B. 2002. *Fit of an axisymmetrical body shape by trigonometric functions*. Private communication.

Pozrikidis, C. 1990. The instability of a moving viscous drop. *J. Fluid Mechanics*, **210**, 1–21.

Stone, H. A., & Leal, L. G. 1989. Relaxation and breakup of an initially extended drop in an otherwise quiescent fluid. *J. Fluid Mechanics*, **198**, 399–427.

Tavares, M. 1992. *Simulation de la déformation d'un domaine fluide en mouvement dans un autre fluide par la méthode des éléments de frontière*. Ph.D. thesis, Institut National Polytechnique de Grenoble, France.

White, F. M. 1991. *Viscous fluid flow*. McGraw Hill.

Zagustin, K. 1992. *An experimental investigation on the deformation of a fluid particle translating in an infinite viscous medium*. Internal note, DTP/SETEX, CEA/Grenoble, France.